

Magnetic interference patterns in a long SNS junction: analytical results

B. Crouzy and D. A. Ivanov

Institute for Theoretical Physics, École Polytechnique Fédérale de Lausanne (EPFL), CH-1015 Lausanne, Switzerland

(Dated: July 1, 2009)

We study a diffusive superconductor–normal metal–superconductor (SNS) junction in an external magnetic field. In the limit of a long junction, we find that the properties of such a system depend on the width of the junction relative to the length associated with the magnetic field. We compute the critical width separating the regime of pure decay (narrow junction) and the regime of damped oscillations (wide junction) of the critical current as a function of the magnetic flux through the junction. We find an exponential damping of the current, different from the well known Fraunhofer limit which corresponds to the limit of a tunnel junction. In the limit of a wide junction, the superconducting pair correlations and the critical current become localized near the border of the junction.

I. INTRODUCTION

The interplay between magnetism and superconductivity in proximity structures results in a rich physics. The experimental observation of the reversal of the critical current (π coupling) in Josephson junctions with a ferromagnetic interlayer^{1,2,3} has recently triggered a lot of interest in the study of the competition between the ferromagnetic and the superconducting order.⁴ Ferromagnetism has also allowed to generate triplet superconducting pair correlations in proximity structures.⁵ Others studies have focused on the Zeeman effect of an external magnetic field in such systems (see for example Ref. 6) and on the possibility to obtain a π junction by applying a field.⁷

In this work, we address the orbital effect of an external magnetic field in a superconductor-normal metal–superconductor (SNS) Josephson junction. Most of the experimental applications cited in the previous paragraph concern diffusive materials, for which an appropriate formalism has been derived.⁸ In the diffusive regime, the motion of the electrons is governed by frequent scattering on impurity atoms: the elastic mean free path l_e is much smaller than the relevant length scales of the system and the Green function becomes isotropic. In many situations, this allows to apply simple one-dimensional models to study the proximity effect. However, including orbital effects in the formalism forbids reducing the system to one dimension. As a result, the proximity effect in the presence of the orbital effect of the magnetic field has been studied until now essentially numerically or in simple limits (wide and short junction or narrow junction) for diffusive hybrid structures^{9,10} and in the clean limit.¹¹

It is well established that in the limit of a thin (tunnel) junction the Josephson current changes sign along the transverse direction and that the total current exhibits a Fraunhofer-like dependence on the magnetic flux through the junction.¹² Observation of this type of dependence has been extensively used experimentally to confirm the Josephson nature of the coupling between superconductors. More recently, shifted Fraunhofer patterns have also served as an indicator for the presence of a net magnetization when a ferromagnetic interlayer is used.^{13,14} It has been then shown both experimentally¹⁵ and theoretically^{9,10} that in proximity structures, discrepancies from the usual Fraunhofer patterns can be present. In particular, the authors of Refs. 9,10 have discussed numerically how the damped oscillatory behavior (Fraunhofer like) characterizing wide and short junctions is replaced by a monotonic exponential decay in narrow junctions. They have also identified the length scale over which the transition between the two regimes takes place.

Motivated by this recent activity and by the rarity of analytical results on the Usadel equation for non one-dimensional geometries, we revisit the problem of the diffusive SNS junction in an external magnetic field. We consider the limit of a long junction and linearized Usadel equations to obtain analytical results for a two dimensional problem. We show that for a narrow junction, the Josephson critical current decays exponentially as a function of the flux through the junction. We find the transition point (the critical width of the junction) where this monotonic decay is replaced by damped oscillations of the critical current. Finally, in the limit of a wide junction, we find damped oscillations with the same period as in the Fraunhofer limit but an exponential decay instead of the purely algebraic decay characterizing Fraunhofer patterns. In this regime, the superconducting correlations become localized in a small region close to the border of the junction. The method we develop does not rely crucially on the choice of particular boundary conditions for the interface between the superconductor and the normal metal: it can be applied either to the situation where the SN interfaces are transparent or to systems with finite interface transparency.

The paper is organized as follows. In Section II we describe the SNS Josephson junction we consider and introduce the formalism used throughout the paper. We then compute the superconducting Green function (Section III) and the Josephson current (Section IV) for the SNS junction in a transverse field. In Section V we discuss the applicability conditions of our method and finally in Section VI we summarize our conclusions.

II. SNS JUNCTION IN A TRANSVERSE MAGNETIC FIELD

We consider a SNS junction in a transverse magnetic field. We introduce a coordinate system with the N layer in the yz plane (Fig. 1). The x axis is directed along the junction, and the SN interfaces correspond to the coordinates $x = 0, L_x$. The origin of the y axis is chosen in the middle of the N layer and we denote the width L_y . The system is invariant under translation along the z axis. We take a uniform magnetic field \mathbf{H} directed along the z axis and neglect the screening of the magnetic field by the Josephson currents.²⁷ For simplicity, we further consider that the London length is short compared to the length of the junction L_x and neglect the penetration of the magnetic field in the superconducting electrodes. An exact treatment would require to add twice the London length to L_x in order to get the total flux through the junction.¹⁶

We assume that the normal layer is strongly disordered and the motion of electrons is diffusive. In this regime, the quasiclassical Green functions¹⁷ (averaged over the fast Fermi oscillations and the momentum directions) are given by the solutions to the Usadel equations.⁸

The (nonlinear) Usadel equation in the normal layer takes the form (we follow the conventions used in Ref. 17)

$$\hbar D \hat{\nabla} \left(\check{g} \hat{\nabla} \check{g} \right) - \omega [\hat{\tau}_3, \check{g}] = 0. \quad (1)$$

$D = v_F l_e / 3$ is the diffusion constant with l_e the elastic mean free path and $\omega = (2n + 1) \pi k_B T$ is the Matsubara frequency. The Green function $\check{g} = \begin{pmatrix} G & F \\ -F^\dagger & -G \end{pmatrix}$ is a matrix in the Nambu (particle-hole) space, and $\hat{\tau}_\alpha$ denote the Pauli matrices in this space. The gradient operator $\hat{\nabla}$ contains the vector potential \mathbf{A}

$$\hat{\nabla} \check{g} = \begin{pmatrix} \nabla G & (\nabla - \frac{2ie}{\hbar} \mathbf{A}) F \\ -(\nabla + \frac{2ie}{\hbar} \mathbf{A}) F^\dagger & -\nabla G \end{pmatrix}. \quad (2)$$

We neglect the Zeeman splitting, which, in the case of the transverse magnetic field, has a typically much smaller effect than the vector-potential term, provided the quasiclassical condition $k_F l_e \gg 1$ is satisfied.²⁸

The Usadel equation is supplemented with the normalization condition for the quasiclassical Green function

$$\check{g}^2 = \check{1}. \quad (3)$$

For simplicity, we assume for the moment that the proximity effect is weak (close to the critical temperature of the superconductor) and that the boundary conditions at the interface with the superconductor are rigid (which is the case for the transparent interface, if the normal region is much more disordered than the superconductor).^{18,19,20} We will see in Section V that these assumptions are not crucial and can be relaxed.

Then the Green function can be linearized around the normal-metal solution as

$$\check{g} = \begin{pmatrix} \text{sgn}(\omega) & F \\ -F^\dagger & -\text{sgn}(\omega) \end{pmatrix}, \quad (4)$$

and, choosing the gauge $\mathbf{A} = -y H \mathbf{e}_x$, the linearized Usadel equation (1) takes the form^{9,10}

$$\left[(\nabla_x + 2i\pi y)^2 + \nabla_y^2 - \frac{|\omega| \xi_H^2}{\hbar D} \right] F(x, y) = 0. \quad (5)$$

Here we have rescaled both coordinates x and y in the units of the magnetic length

$$\xi_H = \sqrt{\frac{\phi_0}{H}}, \quad (6)$$

where $\phi_0 = h/2e$ is the (superconducting) flux quantum. This equation is supplemented by the boundary conditions at the interface with the superconductor and at the open interface,

$$F(x = \{0, L_x\}, y) = F_B e^{\pm i\chi}, \quad (7)$$

$$\nabla_y F(x, y = \pm L_y/2) = 0. \quad (8)$$

The boundary condition (7) is the rigid one, with F_B being the bulk value of the anomalous Green function in the superconductor (close to the superconducting transition temperature, $F_B = \Delta/|\omega|$). The phase difference across the junction is thus denoted 2χ . Condition (8) expresses the vanishing of the current through the interface with vacuum.

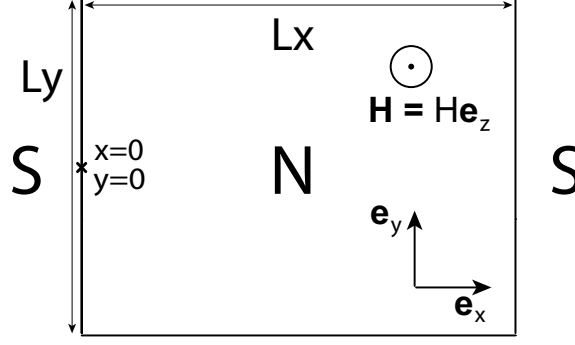


FIG. 1: SNS junction in a transverse magnetic field.

The second anomalous component $F^\dagger(x, y)$ is the complex conjugate of $F(x, y)$. The current density can be calculated from $F(x, y)$ as¹⁷

$$\mathbf{J} = 2\pi i e N(0) D T \sum_{n=0}^{\infty} \left[F^\dagger \nabla F - F \nabla F^\dagger - \frac{4ie\mathbf{A}}{\hbar} F F^\dagger \right] \quad (9)$$

where $N(0)$ is the density of states in the normal metal phase (per one spin projection). The symmetry of translation along the z direction implies that the current remains in the xy plane. The sum is taken over the Matsubara frequencies ω .

III. ANALYTICAL RESULTS FOR A LONG JUNCTION

We are interested in solving the Usadel equation (5) in the middle of the long junction: $L_x \gg \xi_H$. This will allow us to retain only the mode with the slowest decay along the x direction from a spectral decomposition of the solution. To simplify our treatment, we assume that the temperature is sufficiently low, compared to the junction length: $\xi_T \gg L_x$, where the thermal length scale is defined as $\xi_T = \sqrt{\hbar D/T}$. This assumption allows us to neglect the ω term in the Usadel equation (5). We will comment on this assumption in Section V.

First, notice that in the limit of the long junction (when the junction length L_x is much larger than the characteristic length of the decay of the anomalous Green function F) we can approximate the solution of (5) as a superposition²¹ of the two Green functions for the semi-infinite SN problem

$$F(x, y) \approx F_\infty(x, y)e^{i\chi} + F_\infty(L_x - x, -y)e^{-i\chi} \quad (10)$$

where $F_\infty(x, y)$ is the solution for the SN problem with the semi-infinite normal layer. It obeys the same equation (5) with the same boundary condition (8) and with the second boundary condition (7) replaced by $F_\infty(x = 0, y) = F_B$ and $F_\infty(x \rightarrow \infty, y) = 0$.

It will be convenient to use the Fourier decomposition along the x direction by extending the semi-infinite problem to the whole real axis,

$$\left[(\nabla_x + 2i\pi y)^2 + \nabla_y^2 \right] F_\infty(x, y) = f(y) \delta(x), \quad (11)$$

where the right-hand side accounts for the jump in the derivative of the function at $x = 0$. Taking the Fourier transform, we can rewrite this equation in the integral form

$$F_\infty(x, y) = \int \frac{dk}{2\pi} e^{ikx} \left[\nabla_y^2 - (k + 2\pi y)^2 \right]^{-1} f(y). \quad (12)$$

The function $f(y)$ is fixed self-consistently by the boundary condition $F_\infty(x = 0, y) = F_B$.

At positive x , we can close the integration contour in the upper half-plane, and the poles of the integrand are given by the zero modes of the operator

$$A = \nabla_y^2 - (k + 2\pi y)^2 \quad (13)$$

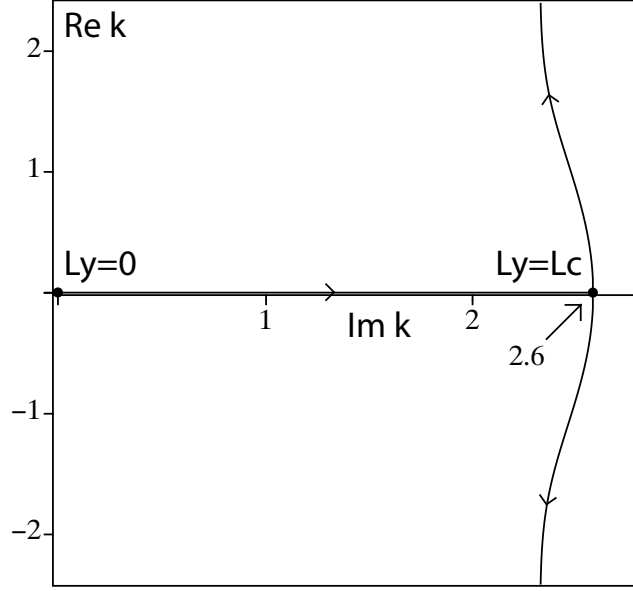


FIG. 2: Effective wave number k , the lengths are given in units of ξ_H . A purely imaginary k indicates a monotonic decay.

(this operator acts on the functions $\psi(y)$ on the interval $-L_y/2 < y < L_y/2$ with the boundary conditions $\psi'(\pm L_y/2) = 0$). In the long-junction limit, the solution in the middle of the junction is determined by the zero mode with the smallest positive imaginary part of k .

The general solution to the second-order differential equation $A\psi = 0$ can be written in terms of a linear combination of two modified Bessel functions,²²

$$\psi = \sqrt{k + 2\pi y} \left(C_1 I_{1/4} \left[\frac{(k + 2\pi y)^2}{4\pi} \right] + C_2 K_{1/4} \left[\frac{(k + 2\pi y)^2}{4\pi} \right] \right). \quad (14)$$

The boundary conditions at $y = \pm L_y/2$ fix the ratio C_1/C_2 and limit the possible values of k to a discrete set.

In Figure 2, we plot the value of k with the smallest positive imaginary part as the width of the junction L_y increases from zero to infinity. In the limit $L_y \rightarrow 0$, the $2\pi y$ correction in the operator (13) may be neglected, and the spectrum is composed of the non-degenerate eigenvalues $k = i n \pi / L_y$ (the “leading” eigenvalue with the smallest imaginary part in the limit $L_y \rightarrow 0$ is thus zero). At a small finite L_y , the leading eigenvalue also becomes finite, but remains purely imaginary. This follows from the combined symmetry of the complex conjugation and the reflection $y \mapsto -y$, which relates the eigenvalues k and $-k^*$. Since the leading eigenvalue is nondegenerate in the limit $L_y \rightarrow 0$, by continuity it must remain purely imaginary for sufficiently small L_y .²⁹

At larger L_y , two imaginary eigenvalues may collide and bifurcate to a pair of complex-conjugate eigenvalues. This happens at $L_y = L_c \approx 0.82$ (see Fig. 2). For $L_y > L_c$, we must take into account the contributions of the two modes (corresponding to the wave vectors k and $-k^*$) since they decay with the same rate (given by the imaginary part of k). In the discussion of the wide-junction limit (Section III.B), we will show that those modes correspond to solutions localized close to the two edges of the junction $y = \pm L_y/2$ (for $L_y \gg 1$). The critical length L_c separates the regime where the superconducting anomalous Green function $F(x, y)$ decays along the x direction without oscillations (narrow junction, purely imaginary k) and the regime where the decay of the Green function is damped oscillatory (wide junction, complex k with both real and imaginary parts).

A. Narrow junction limit

For $L_y \ll 1$ (in the units of ξ_H) we expand the exact solution (14) in powers of L_y and find the wave number k solving the equation for the boundary condition (8) at $y = L_y/2$. This yields the expansion

$$k = \frac{i\pi}{\sqrt{3}} L_y \left(1 + \frac{4\pi^2}{63} L_y^4 + \frac{932\pi^4}{218295} L_y^8 + \frac{7976\pi^6}{13752585} L_y^{12} + \dots \right) \quad (15)$$

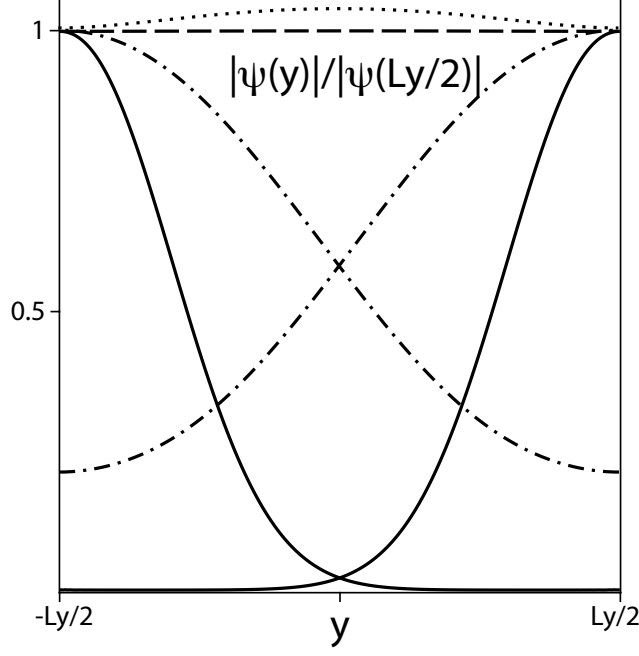


FIG. 3: Superconducting pair correlations $|\psi|$ normalized to their value at the border of the junction for $L_y = 0.25\xi_H$ (dash), $0.75\xi_H$ (dot), ξ_H (dash dot) and $2.5\xi_H$ (solid).

To the lowest order in L_y , the solution to the Usadel equation does not depend on y . In this limit, one can simply average the y^2 term in the Usadel equation (5) and arrive at a pair-breaking term^{9,10,15,23}

$$\frac{\hbar D}{2} \nabla_x^2 F(x) = (|\omega| + 2\Gamma) F(x). \quad (16)$$

with

$$\Gamma = -\frac{\hbar D k^2}{4} = \frac{D e^2 H^2 L_y^2}{12 \hbar}. \quad (17)$$

This result obviously reproduces the first term in (15). For wider junctions, the dependence of the anomalous Green function $F(x, y)$ along the y direction cannot be neglected anymore, but as long as L_y remains smaller than L_c , the function $F(x, y)$ exhibits a monotonic exponential decay along the x direction.

B. Wide junction limit

In the limit of a wide junction $L_y \gg 1$ (as usual, in the units of ξ_H), the solution is determined by the two complex conjugate wave numbers k and $-k^*$. We show below that the asymptotic behavior of k (in the units of ξ_H^{-1}) is

$$k = \pi L_y + k_{\text{res}} \quad (18)$$

where k_{res} is the constant term in the expansion in L_y^{-1} .

Indeed, in the wide junction limit, each of the two zero modes (solutions to $A\psi = 0$) is localized near one of the two edges of the junction and decays quasiclassically towards the other edge. The solution localized near $y = -L_y/2$ should therefore have the quasiclassical wave vector in the operator (13) vanishing in that region, which immediately gives the leading asymptotics $k \approx \pi L_y$ (the solution localized at the opposite edge has $k \approx -\pi L_y$).

To get the subleading term k_{res} , we consider one of those zero modes (say, the one localized near $y = -L_y/2$). This zero mode decays quasiclassically towards the opposite edge of the junction, and with an exponential precision we can replace the boundary condition at $y = L_y/2$ by the decaying condition at infinity, $\psi(y \rightarrow \infty) = 0$. This selects a solution from (14) of the form

$$\psi = \sqrt{k + 2\pi y} K_{1/4} \left[\frac{(k + 2\pi y)^2}{4\pi} \right]. \quad (19)$$

Imposing now the boundary condition $\psi'(-L_y/2) = 0$ implies an equation on k_{res} :

$$K_{3/4} \left[\frac{(k_{\text{res}})^2}{4\pi} \right] = 0. \quad (20)$$

A numerical solution to this equation gives³⁰

$$k_{\text{res}} \approx -1.68 + 2.32i. \quad (21)$$

We illustrate our calculation in Fig. 3, where we plot the zero modes below and above the transition. Below the transition (for $L_x < L_c$), the solution is nondegenerate and symmetric, while above the transition ($L_x > L_c$) the two zero modes are pushed towards the edges of the junction. The characteristic size of the region near the edge where the proximity correlations are localized are of the order 1 [from the solution (19)], i.e., ξ_H in the physical units.

IV. JOSEPHSON CURRENT

The transition between the two types of behavior of the anomalous Green function, purely decaying and decaying with oscillations, may be observed in the critical current of the SNS junction in a magnetic field. Our result on the transition is consistent with the previous numerical works^{9,10}, which indicate that the oscillations appear when the width of the normal region L_y becomes of the order of the magnetic length ξ_H . We show below that the oscillations of the critical current in the SNS system are governed by the same wave vector k as the oscillations of the anomalous Green function $F_\infty(x, y)$ in the SN system discussed in Section III.

In the long-junction limit, the anomalous Green function is given by the expression (10), and, using the expression (9), one arrives at the sinusoidal current-phase relation,²⁴

$$J_{\text{tot}} = I_c \sin 2\chi, \quad (22)$$

where J_{tot} is the total Josephson current (integrated over the y and z directions).

In the “pure decay” regime ($L_y < L_c$), the asymptotic behavior of $F_\infty(x, y)$ is

$$F_\infty(x, y) = F_B \psi(y) e^{ikx} \quad (23)$$

with a purely imaginary k (see Fig. 2), and $\psi(y)$ proportional to the zero mode of the operator (13). This results in the exponential decay of the critical current as a function of L_x :

$$I_c = 8\pi e N(0) D T L_z \left(\sum_{n=0}^{\infty} F_B \right) \frac{1}{i} \left[\int_{-L_y/2}^{L_y/2} (k + 2\pi y) \psi^2(y) dy \right] e^{-|k|L_x}, \quad (24)$$

where L_z is the dimension of the junction along the z direction. Note that this expression is real [since $\psi(y) = \psi^*(-y)$ in this regime] and positive (one checks this numerically).

In the regime of “decaying oscillations” ($L_y > L_c$), the anomalous Green function $F_\infty(x, y)$ contains contributions from two zero modes,

$$F_\infty(x, y) = F_B \left[\psi(y) e^{ikx} + \psi^*(-y) e^{-ik^*x} \right] \quad (25)$$

[here $\psi(y) \neq \psi^*(-y)$ are the two zero modes of the operator (13)]. Integrating the critical current along the y direction, one finds

$$I_c = 8\pi e N(0) D T L_z \left(\sum_{n=0}^{\infty} F_B \right) \text{Im} \left[\int_{-L_y/2}^{L_y/2} (k + 2\pi y) \psi^2(y) dy e^{ikL_x} \right], \quad (26)$$

so that $\text{Im } k$ and $\text{Re } k$ describe the rates of decay and oscillations of the critical current as a function of L_x , respectively. Note that in the case of a wide junction, $L_y \gg \xi_H$, the localization of the superconducting pair correlations at the edge of the junction results in the localization of the superconducting current in the same region.

We sketch the phase diagram of the junction in Fig. 4 in the coordinates L_x and L_y . In experiments, however, one usually varies the external field for a given junction with fixed dimensions. In this setup, the easiest way to observe a transition between the two regimes is to study a junction with $L_x > L_y$ (theoretically, we assume $L_x \gg L_y$, but in practice L_x may be limited by the thermal length ξ_T and by the smallest measurable critical current). In

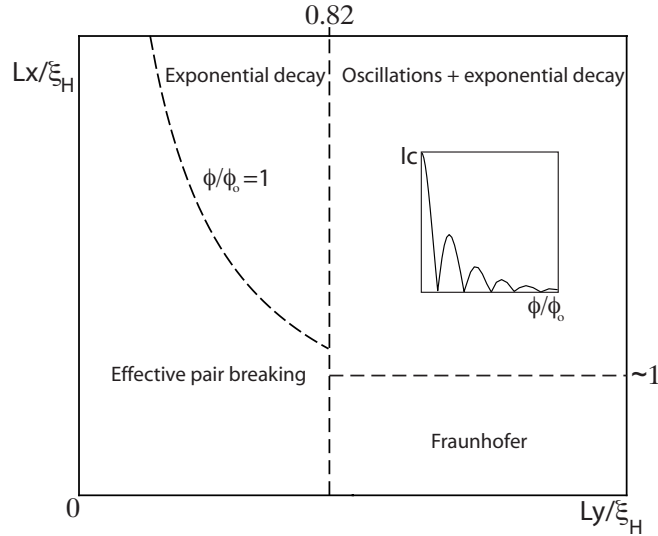


FIG. 4: Phase diagram of the junction in the magnetic field. The left region corresponds to the pure decay regime while in the right one the critical current I_c exhibits interference patterns as a function of the field H .

this case, as the field H increases, one should be able to observe a crossover between the pure-decay regime and the decaying-oscillating regime as ξ_H crosses over L_y . At low fields (for $\xi_H \gg L_y$), in the pure-decay regime, the field dependence of the critical current is

$$I_c = I_1 \frac{\phi}{\phi_0} \exp\left(-\frac{\pi}{\sqrt{3}} \frac{\phi}{\phi_0}\right) \quad (27)$$

where I_1 is of the order of the critical current in the absence of the field [and we have used the leading term in the asymptotics (15)]. This expression reproduces the existing result for a SNS junction with a finite depairing rate (17) [in our treatment, the approximation (10) implies assuming $\phi \gg \phi_0$]²⁵

$$I_c = I_0 \frac{\frac{\pi}{\sqrt{3}} \frac{\phi}{\phi_0}}{\sinh\left(\frac{\pi}{\sqrt{3}} \frac{\phi}{\phi_0}\right)} \quad (28)$$

with I_0 the critical current in the absence of the field. Note that equation (28) is valid only for linearized Usadel equations while we will show in Section V that the domain of validity of the asymptotics (27) can be extended to non-linear situations. At high fields (for $\xi_H \ll L_y$), the critical current exhibits the decaying-oscillating behavior with

$$I_c = I_2 \frac{L_x}{L_y} \exp\left[-2.32 \frac{L_x}{\xi_H}\right] \sin\left[\frac{\pi\phi}{\phi_0} - 1.68 \frac{L_x}{\xi_H} + \varphi_0\right]. \quad (29)$$

Here I_2 is of the same order as I_1 and I_0 (the current in the absence of the external field), $\phi = HL_x L_y$ is the total flux through the junction, and φ_0 is a phase shift, which we do not compute here. Note that while both expressions (27) and (29) decay exponentially with increasing the field, the expression in the exponent of (27) is proportional to H , while that in the exponent of (29) only to \sqrt{H} .

If, however, one considers the current-field dependence for a contact with $L_x < L_y$, then one would observe a crossover from the Fraunhofer pattern (for $\xi_H \gg L_x$)^{9,10,15}

$$I_c = I_0 \frac{\sin(\pi\phi/\phi_0)}{\pi\phi/\phi_0} \quad (30)$$

directly to the wide-junction regime (29), as the magnetic length ξ_H becomes shorter than L_x .

V. APPLICABILITY OF THE RESULTS

To simplify our discussion, we have considered in Sections II–IV the linearized problem with rigid boundary conditions. However, our method is based on finding the zero modes of the operator (13) which describes the proximity

effect in the middle of the junction. Therefore, our results remain valid for more general boundary conditions and for the non-linear case, as long as the junction is sufficiently long (so that the Green function $F_\infty(x, y)$ decays by a factor much larger than one by the middle of the junction). In this case, the Usadel equation close to the middle of the junction can be linearized anyway, and our treatment of Section III can be performed in a similar way, albeit with more complicated boundary conditions. Therefore all the conclusions of Sections III and IV about the different interference patterns of the critical current and about the transition value $L_c \approx 0.82\xi_H$ remain valid. The crucial condition for applicability of our method is thus that the junction is much longer than ξ_H [in the narrow-junction limit, we also need to assume that $\phi \gg \phi_0$ for applicability of our asymptotic formula (27)]. The only role of the boundary conditions and of the non-linearity of Usadel equations is the renormalization of the overall coefficients in the asymptotics (27) and (29).

Another approximation used in our calculation is the assumption of low temperature. As we have seen in the previous sections, the characteristic scale at which the anomalous Green function $F(x, y)$ varies is of the order ξ_H . Therefore, the assumption of low temperature [neglecting ω term in the Usadel equation (5)] implies $\xi_T \gg \xi_H$. Under this low-temperature assumption, the temperature enters only as small corrections to the calculations in the previous sections (including corrections to the zero-mode wave vector k).

We can now qualitatively discuss the high-temperature regime $\xi_T < \xi_H$. In this case, the decay of the anomalous Green function $F(x, y)$ along the x direction is determined mostly by ξ_T , rather than ξ_H , and, as a result, the critical current contains an exponential factor $\exp(-\kappa L_x)$ with $\kappa \approx \sqrt{\pi}\xi_T^{-1}$. However, one can still repeat much of the reasoning of section III in the presence of the ω term. One then finds that in the limit $L_x \rightarrow \infty$, even at high temperature, one can still distinguish the two regimes of the purely decaying and oscillatory-decaying L_x dependence. The critical width L_c separating the two regimes is slightly decreased as compared to the low-temperature case: a dimensional estimate gives $L_c \propto \xi_H^{2/3}\xi_T^{1/3}$ at $\xi_T \ll \xi_H$. On the other hand, the same dimensional estimate indicates that the field contribution to the decay rate along the x direction is of the order $\xi_T^{1/3}\xi_H^{-4/3}$, which translates to a crossover from the purely Fraunhofer regime to the oscillatory-decaying regime at $L_x \sim \xi_H^{4/3}\xi_T^{-1/3}$, i.e. for slightly thicker junctions than at low temperatures.

VI. SUMMARY

To summarize, we consider a long diffusive SNS junction in an external magnetic field \mathbf{H} . We show that depending on the width of the junction relative to the magnetic length $\xi_H = \sqrt{\phi_0/H}$ two different regimes can be observed. For narrow junctions the anomalous Green function F decays monotonically along the junction while for wide junctions exponentially damped oscillations are present. We find that the transition between the two regimes occurs for a width $L_c \approx 0.82\xi_H$. Those different behaviors translate in a monotonic decay of the Josephson critical current (24) as a function of the magnetic flux through a narrow junction and in damped current oscillations for wide junctions. Finally, we show that for wide links the current and the superconducting pair correlations are concentrated in a small region of size ξ_H close to the border of the junction.

The main finding of the present work, in comparison with previous studies of this problem, is the identification of the damped-oscillating phase for wide and long junctions. This phase resembles both the Fraunhofer regime (for wide and short junctions) and the damped phase (for narrow and long junctions). The period of oscillations is the same as in the Fraunhofer interference pattern, while the exponentially decaying factor resembles the damped phase.

Conceptually, the transition between the two asymptotic regimes for long junctions in our problem is similar to the transition between the two regimes in superconductor-ferromagnet-superconductor junctions with domains studied in one of our earlier papers.²⁶ In both systems, the transition between the purely damped and damped-oscillating behavior is related to a bifurcation of the solution to the linearized Usadel equations.

Experimentally the limit of a long junction is accessible and has been the subject of recent experiments.¹⁵ While the decaying regime has been observed, even though without a good quantitative agreement with the theory, the regime of decaying oscillations predicted in our present paper has not been reached, because the fields were not sufficiently high. In future experimental studies, it may be convenient to use junctions with the aspect ratio $L_x/L_y \sim 1$ to access this new damped-oscillating regime, in order to be able to use lower fields than for $L_x/L_y \gg 1$ junctions. In any case, an accurate analysis would be required to distinguish the decaying exponential regime predicted in our paper from the distorted Fraunhofer pattern due to possible structural inhomogeneities of the critical current, as discussed in Ref. 16.

Acknowledgments

This work was supported by the Swiss National Foundation. We thank M. Skvortsov and S. Tollis for helpful discussions.

-
- ¹ V. V. Ryazanov, V. A. Oboznov, A. Y. Rusanov, A. V. Veretennikov, A. A. Golubov, and J. Aarts, Phys. Rev. Lett. **86**, 2427 (2001).
 - ² V. V. Ryazanov, V. A. Oboznov, A. S. Prokofiev, V. V. Bolginov, and A. K. Feofanov, J. Low Temp. Phys. **136**, 385 (2004).
 - ³ V. A. Oboznov, V. V. Bol'ginov, A. K. Feofanov, V. V. Ryazanov, and A. I. Buzdin, Phys. Rev. Lett. **96**, 197003 (2006).
 - ⁴ A. I. Buzdin, Rev. Mod. Phys. **77**, 935 (2005).
 - ⁵ F. S. Bergeret, A. F. Volkov, and K. B. Efetov, Rev. Mod. Phys. **77**, 1321 (2005).
 - ⁶ P. M. Ostrovsky, Y. V. Fominov, and M. V. Feigel'man, Phys. Rev. B **74**, 104505 (2006).
 - ⁷ M. S. Crosser, J. Huang, F. Pierre, P. Virtanen, T. T. Heikkilä, F. K. Wilhelm, and N. O. Birge, Phys. Rev. B **77**, 014528 (2008).
 - ⁸ K. D. Usadel, Phys. Rev. Lett. **25**, 507 (1970).
 - ⁹ J. C. Cuevas and F. S. Bergeret, Phys. Rev. Lett. **99**, 217002 (2007).
 - ¹⁰ F. S. Bergeret and J. C. Cuevas, J. Low Temp. Phys. **153**, 304 (2008).
 - ¹¹ G. Mohammadkhani, M. Zareyan, and Y. M. Blanter, Phys. Rev. B **77**, 014520 (2008).
 - ¹² B. D. Josephson, Rev. Mod. Phys. **36**, 216 (1964).
 - ¹³ J. P. A. A. Bannykh, V. S. Stolyarov, I. E. Batov, V. V. Ryazanov, and M. Weides, Phys. Rev. B **79**, 054501 (2009).
 - ¹⁴ T. S. Khaire, W. P. P. Jr., and N. O. Birge, Phys. Rev. B **79**, 094523 (2009).
 - ¹⁵ L. Angers, F. Chiodi, G. Montambaux, M. Ferrier, S. Guéron, H. Bouchiat, and J. C. Cuevas, Phys. Rev. B **77**, 165408 (2008).
 - ¹⁶ A. Barone and G. Paterno, *Physics and Applications of the Josephson Effect* (Wiley, New York, 1982).
 - ¹⁷ N. Kopnin, *Theory of nonequilibrium superconductivity* (Oxford University Press, 2001).
 - ¹⁸ A. Zaitsev, Zh. Eksp. Teor. Fiz. **86**, 1742 (1984), [Sov. Phys. JETP **59**, 1015 (1984)].
 - ¹⁹ M. Y. Kupriyanov and V. F. Lukichev, Zh. Eksp. Teor. Fiz. **94**, 139 (1988), [Sov. Phys. JETP **67**, 1163 (1988)].
 - ²⁰ A. Altland, B. D. Simons, and D. Taras-Semchuk, Adv. Phys. **49**, 321 (2000).
 - ²¹ D. A. Ivanov, R. von Roten, and G. Blatter, Phys. Rev. B **66**, 052507 (2002).
 - ²² M. Abramowitz and I. A. Stegun, *Handbook of Mathematical Functions with Formulas, Graphs, and Mathematical Tables* (New York: Dover, 1972).
 - ²³ B. Crouzy, E. Bascones, and D. A. Ivanov, Phys. Rev. B **72**, 092501 (2005).
 - ²⁴ A. A. Golubov, M. Y. Kupriyanov, and E. Il'ichev, Rev. Mod. Phys. **76**, 411 (2004).
 - ²⁵ G. Montambaux, arXiv:0707.0411v1 (unpublished) (2007).
 - ²⁶ B. Crouzy, S. Tollis, and D. A. Ivanov, Phys. Rev. B **76**, 134502 (2007).
 - ²⁷ This assumption is justified in most experimental situations with sufficiently weak critical currents, see, e.g., Refs. 7,9,10 for estimates.
 - ²⁸ The Zeeman term may be added as the contribution $\pm i\mu\mathbf{H}$ to the Matsubara frequency in the Usadel equation (1). On the other hand, the characteristic dimensions of the junction for observing the orbital effects discussed in our paper are of the order of the magnetic length (6).^{6,10} One can check that, for $L_x \sim \xi_H$, the Zeeman splitting is much smaller than the Thouless energy $E_{\text{Th}} = \hbar D/L_x^2$ (using the quasiclassical assumption $k_F l_e \gg 1$) and thus may be neglected for most purposes.
 - ²⁹ We thank M. Skvortsov for pointing to us this symmetry.
 - ³⁰ The Macdonald function $K_{3/4}(z)$ does not have zeros on the principal sheet of the Riemann surface, therefore the solution must have $\pi/2 < |\arg k| < \pi$. We also impose the condition $\text{Im } k > 0$, for the mode decaying along the x direction. Finally, under these constraints, we select the root with the smallest imaginary part. Technically, the second sheet of the Riemann surface may be accessed with the relation $K_{3/4}(e^{i\pi}z) = e^{-3\pi i/4}K_{3/4}(z) - i\pi I_{3/4}(z)$.